

AD-A048 064

NAVAL SURFACE WEAPONS CENTER WHITE OAK LAB SILVER SP--ETC F/G 11/6
THE DENSITY, ELECTRICAL RESISTIVITY AND HALL COEFFICIENT OF LI--ETC(U)
SEP 77 M A MITCHELL, R A SUTULA
NSWC/WOL-TR-77-144

UNCLASSIFIED

NL

AD
A048064

END
DATE
FILMED

78

DDC

AD A 048064

NSWC/WOL TR 77-144

12
B-5

THE DENSITY, ELECTRICAL RESISTIVITY AND HALL COEFFICIENT OF Li-B ALLOYS

BY M. A. MITCHELL
R. A. SUTULA

RESEARCH AND TECHNOLOGY DEPARTMENT

23 SEPTEMBER 1977

Approved for public release; distribution unlimited.

DDC
RECEIVED
JAN 5 1978
D

AD No. _____
DDC FILE COPY



NAVAL SURFACE WEAPONS CENTER

Dahlgren, Virginia 22448 • Silver Spring, Maryland 20910

UNCLASSIFIED

SECURITY CLASSIFICATION OF THIS PAGE (When Data Entered)

REPORT DOCUMENTATION PAGE		READ INSTRUCTIONS BEFORE COMPLETING FORM
1. REPORT NUMBER 14 NSWC/WOL-TR-77-144	2. GOVT ACCESSION NO.	3. RESIDENTIAL CATALOG NUMBER <i>Final technical rept. 1 Jul 72-1 Jan 73</i>
4. TITLE (And Subtitle) 6 The Density, Electrical Resistivity and Hall Coefficient of Li-B Alloys.	5. TYPE OF REPORT & PERIOD COVERED Final TR 7/1/72 7/1/72 - 1/1/77	
7. AUTHOR(s) 16 M. A. Mitchell R. A. Sutula		6. PERFORMING ORG. REPORT NUMBER
9. PERFORMING ORGANIZATION NAME AND ADDRESS Naval Surface Weapons Center White Oak Laboratory, Metallic Materials Branch White Oak, Silver Spring, Maryland 20910		8. CONTRACT OR GRANT NUMBER(s) 16 F54594 17 SF54594593
11. CONTROLLING OFFICE NAME AND ADDRESS		10. PROGRAM ELEMENT, PROJECT, TASK AREA & WORK UNIT NUMBERS 6761N; SF54-594-593; 2041; WA07EA
14. MONITORING AGENCY NAME & ADDRESS (if different from Controlling Office)		12. REPORT DATE 11 23 Sep 1977
		13. NUMBER OF PAGES 12 37p.
		15. SECURITY CLASS. (of this report) UNCLASSIFIED
		15a. DECLASSIFICATION/DOWNGRADING SCHEDULE
16. DISTRIBUTION STATEMENT (of this Report) Approved for public release; distribution unlimited		
17. DISTRIBUTION STATEMENT (of the abstract entered in Block 20, if different from Report)		
18. SUPPLEMENTARY NOTES This report, excluding Table 1 and the paragraphs describing the preparation of Li-B and incidental remarks, is accepted for publication in J. Less-Common Metals.		
19. KEY WORDS (Continue on reverse side if necessary and identify by block number) Li-B Compounds Li-rich Li-B Alloys Electrical Resistivity Hall Coefficient Density		
20. ABSTRACT (Continue on reverse side if necessary and identify by block number) The density, electrical resistivity, and Hall constant of LiB Alloys in the concentration range 0-60 at % B are reported. An analysis of the measured density of the LiB reveals that in the composition range 0-40 at % B most of the B is present in a Li-rich phase, probably Li ₅ B ₄ . The electrical resistivity at room temperature was roughly constant between 0 and 45 at % B and then started to rise rapidly with increasing B. The Hall coefficient at room temperature was fairly constant from 0 to 40 at % B and then started to rise. The temperature dependence and magnitude of the electrical resistivity were		

DD FORM 1 JAN 73 1473

EDITION OF 1 NOV 65 IS OBSOLETE
S/N 0102-014-6601

UNCLASSIFIED

SECURITY CLASSIFICATION OF THIS PAGE (When Data Entered)

391596

Inver

UNCLASSIFIED

SECURITY CLASSIFICATION OF THIS PAGE(When Data Entered)

metallic in nature, and there was no evidence of semiconducting behavior at higher B concentrations. There was a break in the resistivity of the 40 at % B sample at the melting point of Li indicating the presence of free Li, but not in the 50 to 60 at % B samples. It was possible to calculate the stoichiometry and density of the LiB phase (or phases) present in the 40 at % B sample: 55.3 at % Li and 1.07 g/cm^3 , respectively, very close to the 55.6 at % Li and 1.0537 g/cm^3 calculated for Li_5B_4 predicted from a recent x-ray and neutron diffraction structure study by Wang, et. al.

↖

CC

UNCLASSIFIED

SECURITY CLASSIFICATION OF THIS PAGE(When Data Entered)

SUMMARY

The density, electrical resistivity, and Hall constant of LiB alloys in the concentration range 0-60 at % B are reported. The binary phase diagram of this system has not been reported in the literature and the data presented here are used to obtain information about the phases present. An analysis of the measured density of the LiB reveals that in the composition range 0-40 at % B most of the B is present in a Li-rich phase, probably Li_5B_4 , with possibly some Li_3B also present. Up to 40 at % B there are also significant amounts of free Li in these alloys. The electrical resistivity at room temperature was roughly constant between 0 and 45 at % B and then started to rise rapidly with increasing B. The Hall coefficient at room temperature was fairly constant from 0 to 40 at % B and then started to rise. The temperature dependence and magnitude of the electrical resistivity were metallic in nature, and there was no evidence of semiconducting behavior at the higher B concentrations. There was a break in the resistivity of the 40 at % B sample at the melting point of Li indicating the presence of free Li, but not in the 50 to 60 at % B samples. It was possible to calculate the stoichiometry and density of the LiB phase (or phases) present in the 40 at % B sample: 55.3 at % Li and 1.07 g/cm^3 , respectively, very close to the 55.6 at % Li and 1.0537 g/cm^3 calculated for Li_5B_4 predicted from a recent x-ray and neutron diffraction structure study by Wang, et al.

J R Dixon
J. R. DIXON
By direction

ACCESSION NO.	
NTIS	White Section <input checked="" type="checkbox"/>
DDC	Buff Section <input type="checkbox"/>
UNANNOUNCED	<input type="checkbox"/>
JUSTIFICATION	
BY	
DISTRIBUTION/AVAILABILITY CODES	
Dist.	AVAIL. and/or SPECIAL
A	

DDC
RECEIVED
JAN 5 1978
RECEIVED

CONTENTS

	Page
INTRODUCTION	4
EXPERIMENTAL	6
RESULTS	15
Electrical Resistivity and Hall Constant	15
DENSITY	24
Density, Discussion and Interpretion	24
CONCLUSIONS	31
REFERENCES	33
ACKNOWLEDGEMENTS	34

ILLUSTRATIONS

<u>FIGURE</u>		<u>PAGE</u>
1	Hermetically sealed sample holder for electrical resistivity and Hall coefficient measurements	10
2	Circuit used to measure electrical resistance and Hall voltage of samples	11
3	Sample holder used to make measurement of electrical resistance above room temperature	13
4	Electrical resistivity at room temperature of LiB as a function of B concentration	16
5	Hall constant at room temperature of LiB as a function of B concentration	17
6	Degradation of a 39.1B sample in the hermetically sealed sample holder as a function of time at room temperature	18
7	Electrical resistivity of LiB alloys as a function of temperature	21
8	Density of LiB alloys as a function of concentration of B	25
9	Percentage difference between the measured density d_m , and the calculated density, d , of a mixture of Li with a second phase	29

TABLES

<u>TABLE</u>		<u>PAGE</u>
1	Sample Preparation and Properties	7, 8
2	Comparison of Electrical Data	19
3	Calculation of Stoichiometry of Phase I in 40B Sample	23
4	Possible LiB Compounds	27
5	Composition of LiB with 3 Phases Present, Li, Li_5B_4 and Li_3B	30

INTRODUCTION

Until 1972 there were only scattered and sketchy reports of the existence of LiB compounds, all boron rich. These included: LiB_6 ¹; $\text{Li}_{0.32}\text{B}_{0.68}$ ²; LiB_4 with $a = 7.20\text{\AA}$ and $d = 1.73\text{ g/cm}^3$; ³ and $\text{LiB}_{10.85 \pm 0.35}$ with $a = 7.18\text{\AA}$.⁴ Extensive studies of the properties of these compounds were not made. However, in 1972 a binary alloy system of LiB was discovered⁵, which has quite an interesting binary phase structure at the Li rich compositions. Since the density of Li is only 0.534 g/cm^3 (and B is 2.535 g/cm^3)⁶ these alloys are super-lightweight and in some cases lighter than water. Some of the properties of these Li-rich alloys have been measured. Recently James and Devries⁷ reported the anodic discharge behavior of two of these LiB alloys, containing 13.8B and 31.6B (the numbers refer to atomic concentration of boron) in a LiCl-KCl eutectic melt between 673 and 873°K. Calculated values of the amount of Li contained in the LiB alloy anodes at the main break of the discharge curves clustered around 67 at.% Li. It was suggested that this end product was Li_2B , but our work shows that this could in fact be a mixture of two phases. In other work X-ray and neutron diffraction NMR measurements have recently been completed in the composition range of 0 - 60B⁸. These results indicate that there are two or more phases present in addition to free Li in the alloys in this concentration range and that one of the phases has a stoichiometry of Li_5B_4 and a lattice spacing of 4.935\AA . The calculated density is 1.0537 g/cm^3 (one Li_5B_4 molecule per unit cell). The Li atoms are arranged in a bi-tetrahedral cluster with Li

1. Elliott, R. P., Constitution of Binary Alloys, First Supplement, (McGraw-Hill, New York, 1965), p. 124.
2. Shunk, F. A. Constitution of Binary Alloys, Second Supplement, (McGraw-Hill, New York, 1969), p. 89.
3. Casanova, J., French Patent No. 1,461,878 (1965).
4. Secrist, D. R., "Compound Formation in the Systems Lithium-Carbon and Lithium-Boron," J. Amer. Cer. Soc., 50, 520 (1967).
5. Wang, F. E., "Unusual Phenomenon in the Formation of Li-B Compound Alloy," Naval Surface Weapons Center, White Oak Laboratory, submitted to Phys. Rev. Lett.
6. Gray, Dwight E., American Institute of Physics Handbook, Third Ed., (McGraw-Hill, New York, 1972), pps. 2-19, 2-20.
7. James, S. D. and Devries, L. E., "Structure and Anodic Discharge Behavior of Lithium-Boron Alloys in the LiCl-KCl Eutectic Melt," J. Electrochem. Soc., 123, 321 (1976).
8. Wang, F. E., "The Crystal Structure Study of Li_5B_4 ," NSWC/WOL TR 77-84, (ONR Report No. N-0014-WR0030). 1977.

atoms at the five apices. The four boron atoms are in planar trigonal cluster with 3 boron atoms at the corners and one in the center. The structure is rhombohedral (R3) in its short-range-ordered state and bcc (I23) in the statistically disordered (long range) state. The interatomic distance of the Li atoms is only 1.25Å, which is similar only to that of Li in Li₂ vapor. The small atomic size is also consistent with the density results to be reported in Section III, which indicate a very close packing of Li and B.

Data on the density, Hall coefficient, and electrical resistivity, of LiB as a function of composition, and in the case of electrical resistivity, as a function of temperature, are reported in this article. In a binary alloy at thermodynamic equilibrium at constant pressure only two phases can coexist (Gibbs phase rule). However, there were more than two phases present in the alloys discussed here and hence they were not at equilibrium. Very little was known about the phases present, and thus the data are interpreted in that light. Since the alloys are highly reactive with air, a number of special apparatuses had to be designed and precautions taken to avoid contamination. These are described in Section II. The results of the measurements are presented in Section III and used as much as possible to get information about the metallurgical nature of the alloys. The conclusions are in Section IV.

EXPERIMENTAL

The properties of lithium-rich Li-B alloys are difficult to understand because of the unique way that solid Li-B is formed. Because the boiling point of lithium, 1330°C, is lower than the melting point of boron, 2030°C, the conventional method of preparing Li-B compounds, i.e., heating both constituents together above their melting points, has met with only limited success; only complicated B-rich compounds have been previously prepared. However, the Li-B alloys discussed here were prepared by a different process which results in the formation of lithium-rich compounds also.

The process involves two steps. Molten lithium is extremely reactive (increasingly so as the temperature is raised), and it is found that finely divided, solid boron will dissolve readily in the melt between 180°C and 500°C (with a limit of about 60 a/o B, empirically). Thus, the first step in the preparation involves melting lithium in an iron crucible and dissolving boron while the temperature gradually increases over a period of 1/2 to 2 hours to 500°C. Initially, it appears that there is a lot of free lithium present at the top of the melt and a thicker solution of Li-B and free boron at the bottom of the crucible. As the temperature rises, the melt thickens and the free lithium is eventually absorbed. The appearance of the melt is a shiny, white metallic lustre. As the temperature nears 500°C the melt loses its metallic lustre and becomes white and pasty.

The second step in the preparation process is what gives Li-B its unique place among metallic alloys. As the temperature rises above 500°C, at some temperature below 800°C the Li-B solution goes through a strongly exothermic, irreversible reaction and forms a metallic solid. The kinetics of this alloy formation reaction are not well understood. Once it starts, it cannot be controlled, and because of the violence and speed of the reaction atoms don't have time to diffuse to equilibrium positions; any inhomogeneities in the melt are frozen in. Thus, it is to be expected that these alloy samples will be formed in a state containing several non-equilibrium phases.

All samples discussed here were prepared with 99.9% pure Li (with principal impurities 0.008% Na and 0.006% Fe, by weight) obtained from the Foote Mineral Company and 98.9% pure B (with principal impurities 0.60% C, 0.14% Fe, 0.009% H, 0.015% N, 0.09% O, 0.10% Si, and 0.01% Mg, by weight) obtained from either Atomergic or Kawecki Berylco Industries, Inc., in an iron crucible in a glove box with a helium atmosphere in which each of the individual impurities, O₂, N₂, and H₂O, were less than 1 ppm.

The preparation of the electrical samples is summarized in Table 1, along with the electrical properties measured. In all cases the boron was added to the molten lithium at a temperature of 450°C, and after the transition and anneal 2, the samples were removed from the furnace and allowed to cool in ambient.

TABLE 1

SAMPLE PREPARATION AND PROPERTIES

Dissolution temperature = 450°C

	Nominal Conc. B (at.%)	Boron Sup- plier ^a	Boron Mesh Size	Melt Cond ^b	Anneal #1 ^c		Trans Temp ^d (°C)	Anneal #2 ^e		Surface Sanded?
					Temp (°C)	Time (Hrs)		Temp (°C)	Time (mins)	
1a	9.66	K	-200+300	3	510	1.0	717	----	----	No
1b	9.66	K	-200+300	3	510	1.0	717	----	----	Yes
2	17.63	K	-200+300	2	510	1.0	711	----	----	Yes
3	24.3	K	-200+300	2	510	2.3	711	----	----	Yes
4	32.5	K	-200+300	2	510	1.5	711	----	----	Yes
5	39.1	K	-200+300	2	510	1.0	711	----	----	Yes
6a	39.1	A	-200+300	2	510	1.0	711	----	----	No
6b	39.1	A	-200+300	2	510	1.0	711	----	----	Yes
7	40.0	K	-120+200	2	---	---	700	----	----	Yes
8	42.82	K	-80+120	3	---	---	700	----	----	No
9	42.82	K	-200+300	3	510	1.0	718	718	5	Yes
10	42.82	A	-120+200	2	510	2.1	711	711	5	Yes
11	42.82	A	-120+200	2	510	2.0	711	711	5	Yes
12	45.0	K	-----	-	---	---	700	----	----	Yes
13	46.12	K	-80+120	2	---	---	700	----	----	No
14	46.12	A	-200+300	3	510	1.0	717	----	----	Yes
15	46.12	A	-120+200	2	513	1.0	745	745	5	Yes
16	49.05	K	-80+120	2	---	---	700	----	----	No
17	49.05	K	-80+120	3	---	---	700	----	----	No
18	49.05	K	-120+200	3	---	---	700	----	----	No
19	49.05	A	-200+300	2	525	1.0	711	711	5	Yes
20	49.05	A	-120+200	3	500	1.0	743	743	5	Yes
21	49.05	A	-120+200	1	478	1.5	650	650	10	Yes
22	49.05	A	-120+200	1	478	1.5	650	650	10	Yes
23	49.05	A	-120+200	2	478	1.5	650	650	10	Yes
24	50.0	K	-----	2	---	---	700	----	----	Yes
25a	51.69	K	-80+120	2	---	---	700	----	----	No
25b	51.69	K	-80+120	2	---	---	700	----	----	Yes
26	51.69	K	-120+200	2	556	1.5	556	600	5	No
27	51.69	K	-200+300	2	510	1.0	726	----	----	Yes
28	51.69	K	-200+300	2	510	1.0	711	----	----	Yes
29	51.69	A	-120+300	2	521	1.0	734	734	5	Yes
30a	54.94	A	-120+200	2	---	---	719	----	----	No
30b	54.94	A	-120+200	2	---	---	719	----	----	Yes
31a	54.94	A	-120+200	2	---	---	719	----	----	No
31b	54.94	A	-120+200	2	---	---	719	----	----	Yes
32	58.2	K	-120+200	3	---	---	700	700	3	No
33	60.0	K	-----	2	---	---	700	----	----	Yes

^a K = Kaweck; Berylco Industries; A = Atomergic^b Condition of melt before transferring material into mold

1. Pure liquid lithium still present with molten Li-B
2. Liquid lithium and boron completely combined and viscous
3. Melt pasty

^c Anneal of material after transfer to mold^d Temperature at which sample was mold held to cause transition^e Anneal after transition

TABLE 1 (Cont.)

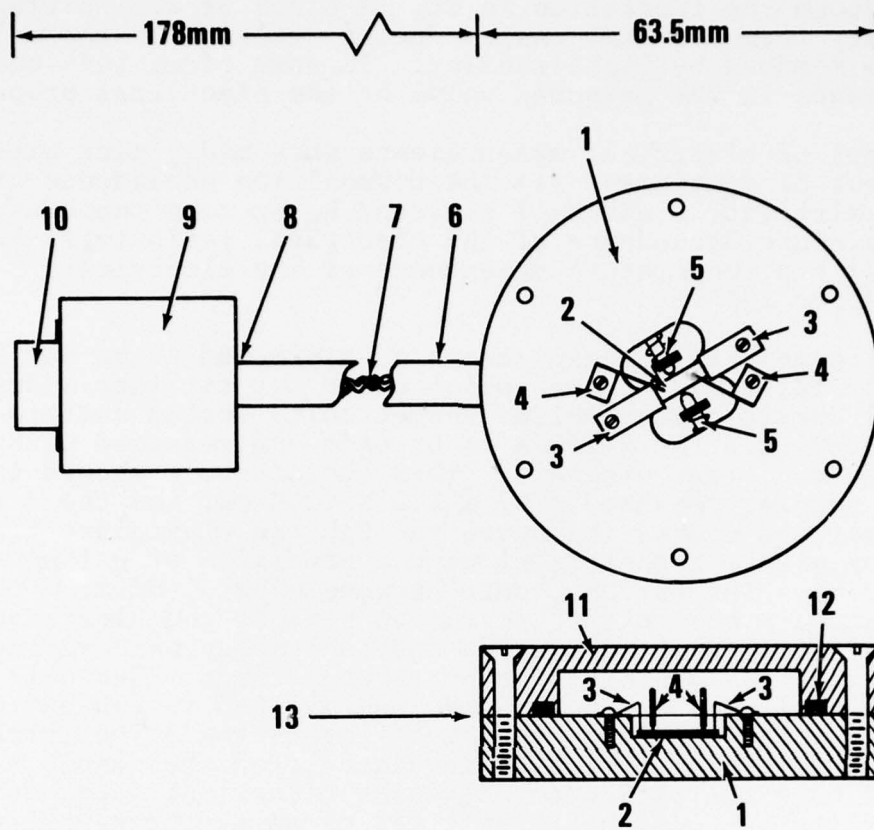
All Samples Cooled Outside of Furnace

Sample No.	Nominal Conc. B (at.%)	ρ ($\mu\Omega\text{cm}$)	R_H ($10^{-10}\text{m}^3\text{c}^{-1}$)	Comments
1a	9.66	13.2	7.27	
1b	9.66	12.4	7.11	Sample 1a with surfaces sanded
2	17.63	13.7	9.40	
3	24.3	12.4	9.41	
4	32.5	13.0	9.51	
5	39.1	13.4	9.82	
6a	39.1	15.8	10.6	
6b	39.1	13.8	9.25	Sample 6a with surfaces sanded
7	40.0	17.1	----	
8	42.82	14.1	10.7	
9	42.82	14.9	10.1	
10	42.82	13.3	8.68	Transition occurred during Anneal 1
11	42.82	21.0	11.3	Transition occurred during Anneal 1
12	45.0	18.4	----	
13	46.12	13.72	11.9	
14	46.12	15.4	10.0	
15	46.12	14.7	9.53	
16	49.05	20.5	8.96	
17	49.05	24.7	11.5	
18	49.05	18.3	11.6	
19	49.05	17.5	11.6	Transition may have occurred during Anneal 1
20	49.05	13.9	9.55	
21	49.05	19.9	12.9	
22	49.05	16.9	9.96	
23	49.05	22.5	12.6	
24	50.0	25.3	----	
25a	51.69	19.30	10.1	
25b	51.69	19.41	9.49	Sample 25a with surfaces sanded
26	51.69	16.38	12.0	Transition occurred during Anneal 1.
27	51.69	23.0	12.0	
28	51.69	18.1	10.4	
29	51.69	18.2	11.3	
30a	54.94	23.2	10.6	
30b	54.94	23.1	10.3	Sample 30a with surfaces sanded
31a	54.94	18.5	10.2	From same melt as sample 30
31b	54.94	18.8	9.7	Sample 31a with surfaces sanded
32	58.2	24.8	11.0	
33	60.0	54.3	----	

Because of the difficulty of machining samples in the glove box, at some point in the process of dissolving boron (indicated in Table 1) part of the material was transferred to a stainless steel sample mold, and taken through the transition in it. A black or grey surface coating usually formed on the sample during reaction in the mold. This could be removed by light sanding. In some cases this coating made a difference in the measured value of the electrical properties.

Three types of electrical measurements were made, each with its own special set of problems: (1) the composition dependence of the electrical resistivity ρ and Hall constant R_H at room temperature; (2) the temperature dependence of the electrical resistivity below 293°K; and (3) the temperature dependence of the electrical resistivity above 293°K.

In order to make Hall measurements a sample had to be put between the poles of a large magnet, one which would not fit into a dry box; thus, a small easily-disassembled, hermetically sealed container was built which permitted the samples to be made and measured without ever coming into contact with air. This container is showed in Fig. 1. The samples measured 9.67 X 2.5 X 0.40 mm, and the distance between the voltage probes (measured through the plexiglass front of the dry box with a cathetometer with a precision of 0.1 mm) was typically 6.0 mm. The current contacts were about 1 mm from the voltage contacts, a sufficient separation because the electrical resistivity of similar sized pure Cu and Ta samples were reproduced within 2% of their values measured by other methods. The Hall voltage contacts in Fig. 1 were spring loaded, and slipped in and out of nylon bushings which provided electrical insulation. The current and voltage contacts were electrically insulated from the sample holder by means of 0.05 mm thick Scotch polyester electrical tape, #65. The sample holder fit between the 10 cm poles of an electromagnet which provided a field of 1.66 T for all Hall measurements. Fig 2 shows the electrical circuit used to measure the Hall coefficient and electrical resistivity. The electrical current (0.2 amp max) was swept through one cycle with a period of 20 secs in both zero magnetic field and with magnetic field in forward and reverse polarities. By sweeping the current this way the effect of thermal emf's and Hall contact offset could be eliminated. The electrical resistivity is $\rho = s \cdot A/L$ where s is the slope of the V_x versus current plot on the X-Y recorder multiplied by appropriate scale factors, and A/L is the geometry factor of the sample. The Hall coefficient $R_H = 0.5\Delta S \cdot t/B$ where ΔS is the difference between slopes of Hall voltage versus current plots on the X-Y recorder for magnetic induction, B , in the forward and the reverse directions, respectively, and t is the sample thickness. The thickness and width of the samples were measured with a micrometer with a precision of 0.0015 mm, but variations in the cross sectional dimensions gave rise to an error of about 3% in the thickness and 1% in the width. The experimental error in measuring the slope of the line from the X-Y recorder was less than 0.3%. Another factor which affected the sample dimensions was an oxide coating deposited during preparation about 0.02 to 0.04 mm thick which had to be sanded off.



- | | |
|--------------------------|-------------------------------|
| 1 Brass Sample Holder | 8 Epoxy Seal (Inside) |
| 2 Sample | 9 Brass Mount |
| 3 Current Contact, Knife | 10 10-pin Connector |
| 4 Voltage Contact, Point | 11 Cover, Section |
| 5 Hall Voltage Contact | 12 O-Ring |
| 6 Copper Tube | 13 Section Along Sample Axis, |
| 7 Electrical Leads | Including Cover |

FIGURE 1 HERMETICALLY SEALED SAMPLE HOLDER FOR ELECTRICAL RESISTIVITY AND HALL COEFFICIENT MEASUREMENTS.

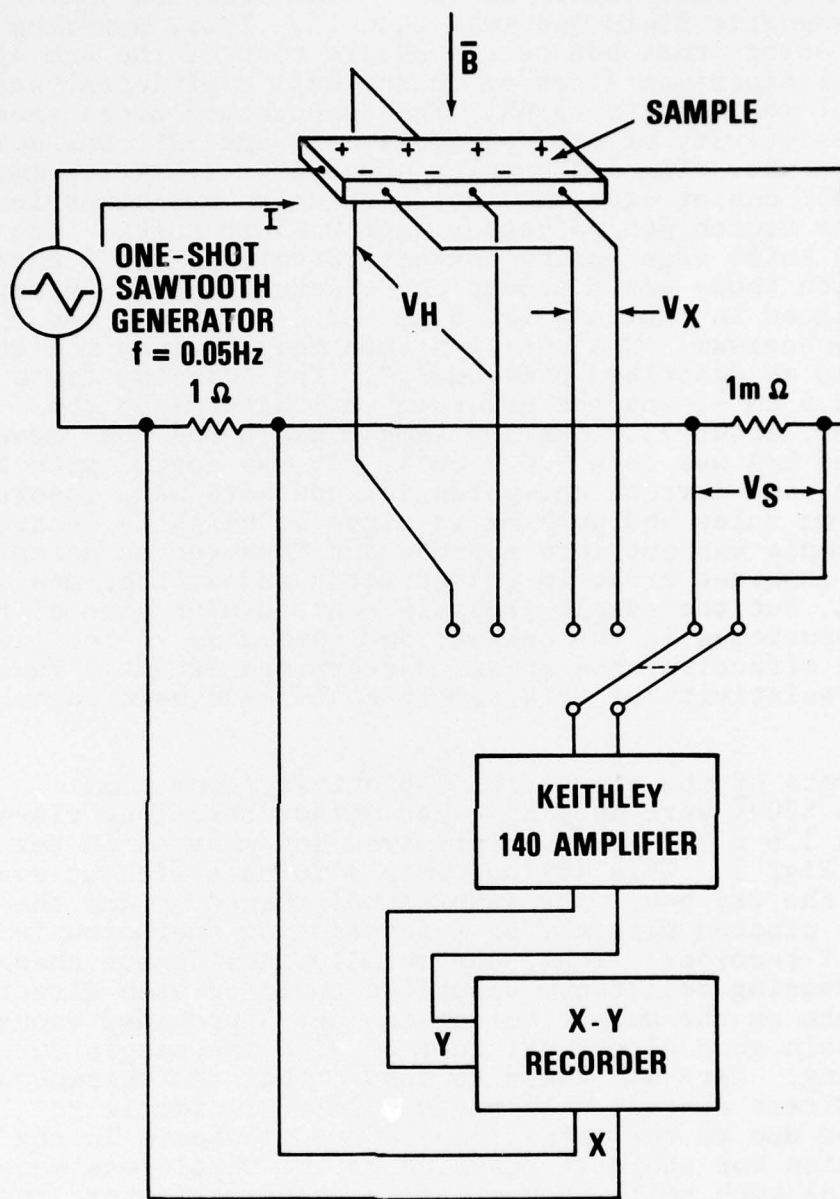


FIGURE 2 CIRCUIT USED TO MEASURE ELECTRICAL RESISTANCE AND HALL VOLTAGE OF SAMPLES

In the case of the Hall coefficient, the difference in slopes could be measured with error of 5% or less. The error of the measurements of magnetic field was less than 1%. Thus, assuming that these are random errors that add as the square root of the sum of the squares, the total experimental error in the Hall coefficient was 6%, and the electrical resistivity, 3.6%. The temperature dependence of the electrical resistivity of two specimens, 45B and 50B, was measured below room temperature. The 45B sample, about 32 x 1.5 x 1.8 mm, was sealed into a small copper case the inside of which was electrically insulated with the Scotch #65 polyester tape 0.05 mm thick. The lid of the case had 4 knife edge spring contact, 2 voltage and 2 current, attached to it with epoxy seals around the electrical feed-throughs. The sample was placed in the case (50.8 mm x 3.2 x 1.5 mm) and the lid sealed on with beeswax. The case was then mounted in a resistance probe and measured as described previously⁹. The geometry factor L/A , was $54.1 \pm 1.5 \text{ cm}^{-1}$, and the error in this determined the experimental error, about 3%. The 50B sample was a rod that measured 76.2 x 4.5 mm, and L/A was $20.4 \pm 0.2 \text{ cm}^{-1}$. It was coated with beeswax after preparation, and current and potential contacts were inserted by drilling 0.79 mm holes and pushing in wires of slightly greater diameter. The sample was put into a probe and measured as described previously⁹. The combined error in the geometry and voltage measurements was only 1%, but the sample probably reacted with some of the oxygen and H_2O impurities in the beeswax and formed an oxide layer which reduced the effective area to an undetermined extent. Thus, the error in the resistivity of this sample could have been rather large.

The measurements of the electrical resistivity from room temperature up to 870°K were made by an AC method described elsewhere¹⁰. The samples (51 x 1.6 x 3.2 mm) were prepared and mounted in the sample holder in Fig. 3. This was put into a furnace without ever removing it from the dry box. The furnace was turned on and the sample resistance plotted directly as a function of thermocouple voltages on an X-Y recorder. Thus, any metallurgical phase changes in the material causing resistance anomalies could be seen directly. The Inconel weights on the sample holder in Fig. 3 provided enough pressure to maintain good electrical contact with the sample during heating and cooling. Care was taken to ensure that the thermocouple junction was in direct contact with the middle of the sample to minimize the error due to the large temperature gradients in the oven. No correction for thermal expansion of the sample was made. This could cause as much as 1% change in the geometry factor, and hence the resistivity over the 273 - 873°K temperature range.

9. Mitchell, M. A., "A Simple Resistance Probe for Measurements from 4.2 to 300K," Rev. Sci. Inst., 45, 708 (1974).

10. Mitchell, M. A., "A Simple Microohmmeter," submitted for publication in Rev. Sci. Inst.

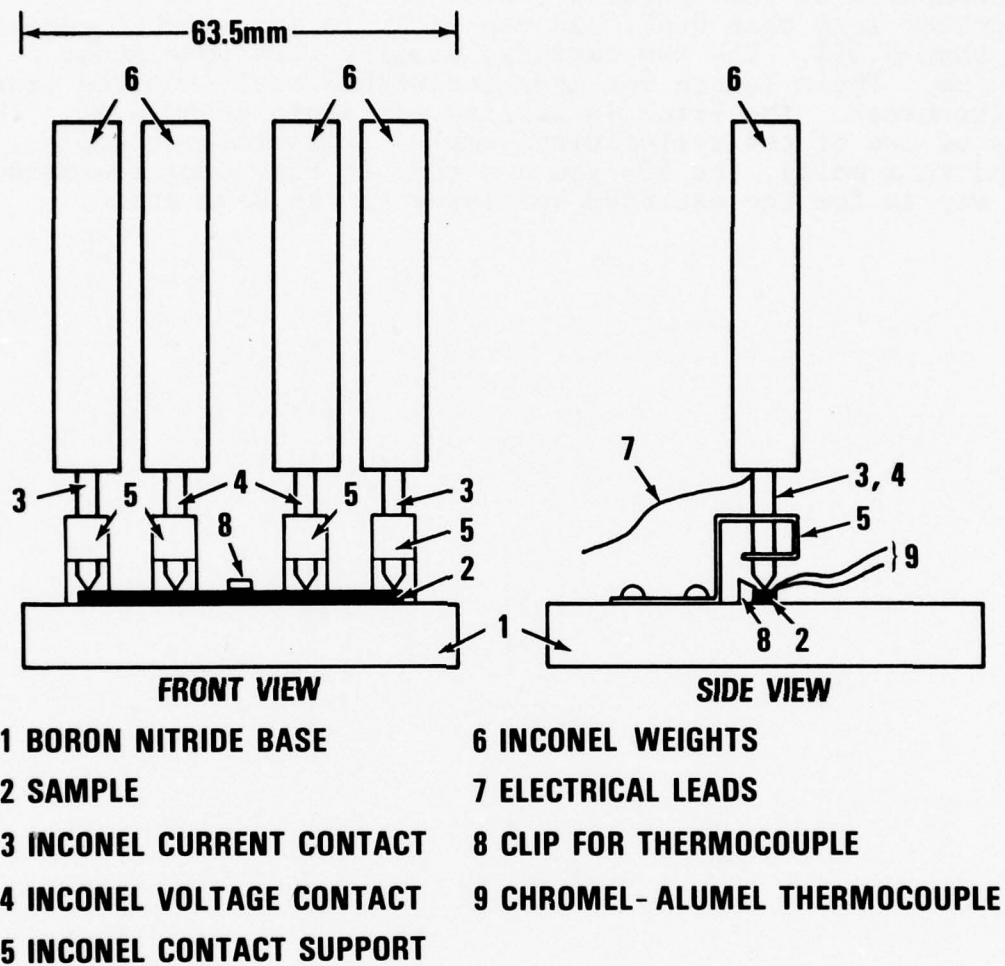


FIGURE 3 SAMPLE HOLDER USED TO MAKE MEASUREMENTS OF ELECTRICAL RESISTANCE ABOVE ROOM TEMPERATURE.

There were nine density specimens. Five of them (the unconstrained specimens) were made in an iron crucible and machined into cylindrical samples about 13 mm long by 28 mm in diameter and 5-13 g in weight. The length and diameter were measured with a micrometer with 2.5 μ m precision, and the weighing was done with a precision of 1 mg. The surface roughness of the specimen caused an error in the volume measurement of less than 0.4%, and the error in the weight measurement was less than 0.05%. The two extruded samples were rods about 6.4 x 100 mm. Their length was measured with a scale and the diameter with a micrometer. The error in density was again about 0.4%. The densities of two of the resistivity samples (constrained samples, solidified in a mold), the 50B rod and the 40B bar, were measured in the same way as for the extruded samples with the same error.

RESULTS

ELECTRICAL RESISTIVITY AND HALL CONSTANT. The results of the electrical resistivity and Hall coefficient measurements are shown in Figs. 4 and 5. In the case of the electrical resistivity the general trend in the data is a gradual increase up to about 45B and then a strong increase above that composition. In Table 2 the room temperature resistivity and Hall coefficient of Li, B, and $\text{Li}_x\text{B}_{1-x}$ are compared with some other metals. Boron has a very high, semiconducting value of electrical resistivity, and Li a low, metallic resistivity. One would expect that in spanning the composition range from pure Li to pure B the alloy would exhibit an increase in electrical resistivity of over 13 orders of magnitude! From Fig. 4 it would seem then that metallic LiB phases become significant between 0 and 10B, and there is a mixture of pure Li with these phases up to about 44B. Above that, other B-rich phases with high electrical resistivities are formed in significant amounts. The electrical resistances of these phases add as resistances in parallel, and the lower resistance phases short out the higher ones.

The Hall data in Fig. 5 show the same general trend, except that the composition region in which the LiB phases become significant is pinpointed somewhat better. The Hall constant of Li (see Table 2) is small and negative, but for B it is large and positive. At 10B the Hall constant of the alloy is already large and positive relative to pure Li. This behavior would have to be attributed to the presence of the LiB phases or pure B, most likely the former because there is no drastic increase of R_H at the higher concentrations of B as would be expected if significant amounts of free B are present.

It can be seen that there is a large amount of scatter in the vicinity of 50B, in both the electrical resistivity and Hall coefficient. It is considerably larger than the experimental error, 4% and 6%, respectively, and is almost certainly caused by variations in the relative amounts of the phases present and porosity, as the density measurements will show later.

Another problem which affects the measurement is the reactivity of these alloys. In order to test the reactivity of the samples in the sample holder the change in ρ and R_H was measured as a function of time, as shown in Fig. 6. Firstly, this shows us that there was not a significant amount of oxidation of the samples between the time the sample holder was sealed, and the time the measurements were made, no more than one-half hour. Secondly, the difference in degradation rates between the electrical resistivity and Hall constant indicates that the two parameters are each characteristic of different phases. The electrical resistivity of the alloy is more characteristic of the pure Li present in the sample, because it has the lowest resistivity. The Hall constant of the alloy is more characteristic of the LiB phases because they are positive and Li is negative. It would seem, then that the LiB phases degrade at a much faster rate than the pure Li.

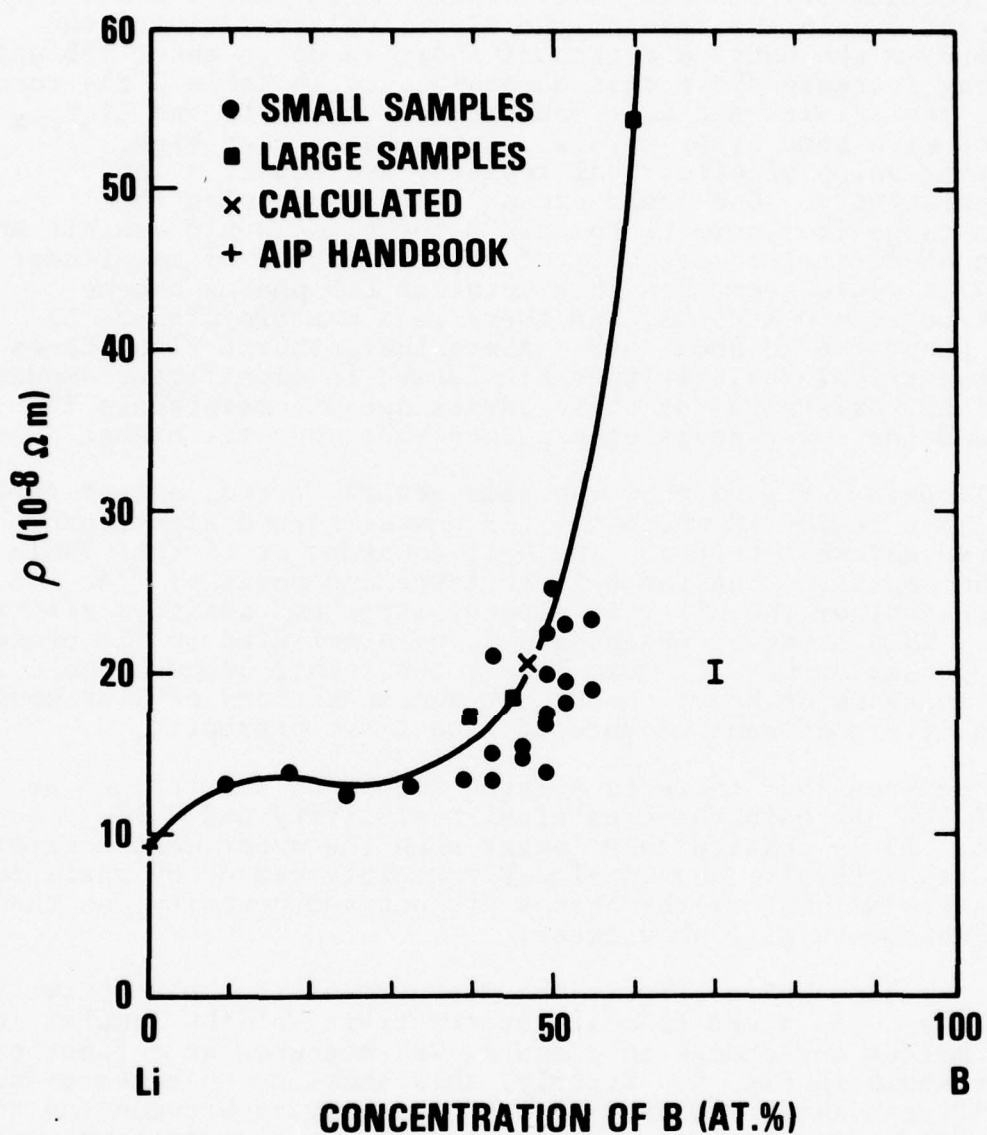


FIGURE 4 ELECTRICAL RESISTIVITY AT ROOM TEMPERATURE OF LiB AS A FUNCTION OF B CONCENTRATION. THE (X), FOR Li_5B_4 , IS CALCULATED FROM THE 40B ALLOY.

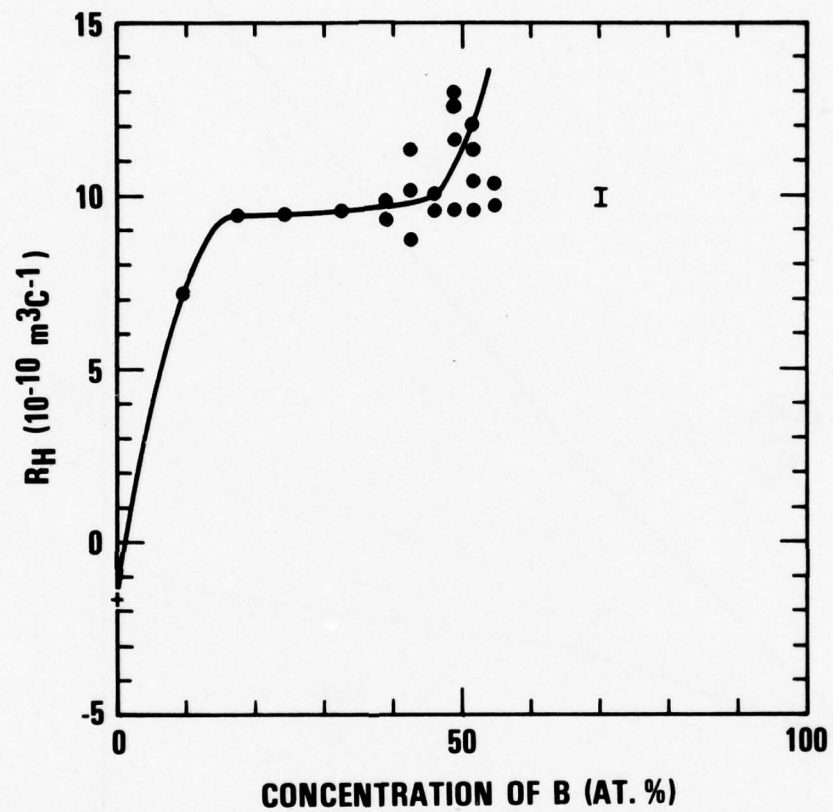


FIGURE 5 HALL CONSTANT AT ROOM TEMPERATURE OF LiB AS A FUNCTION OF B CONCENTRATION.

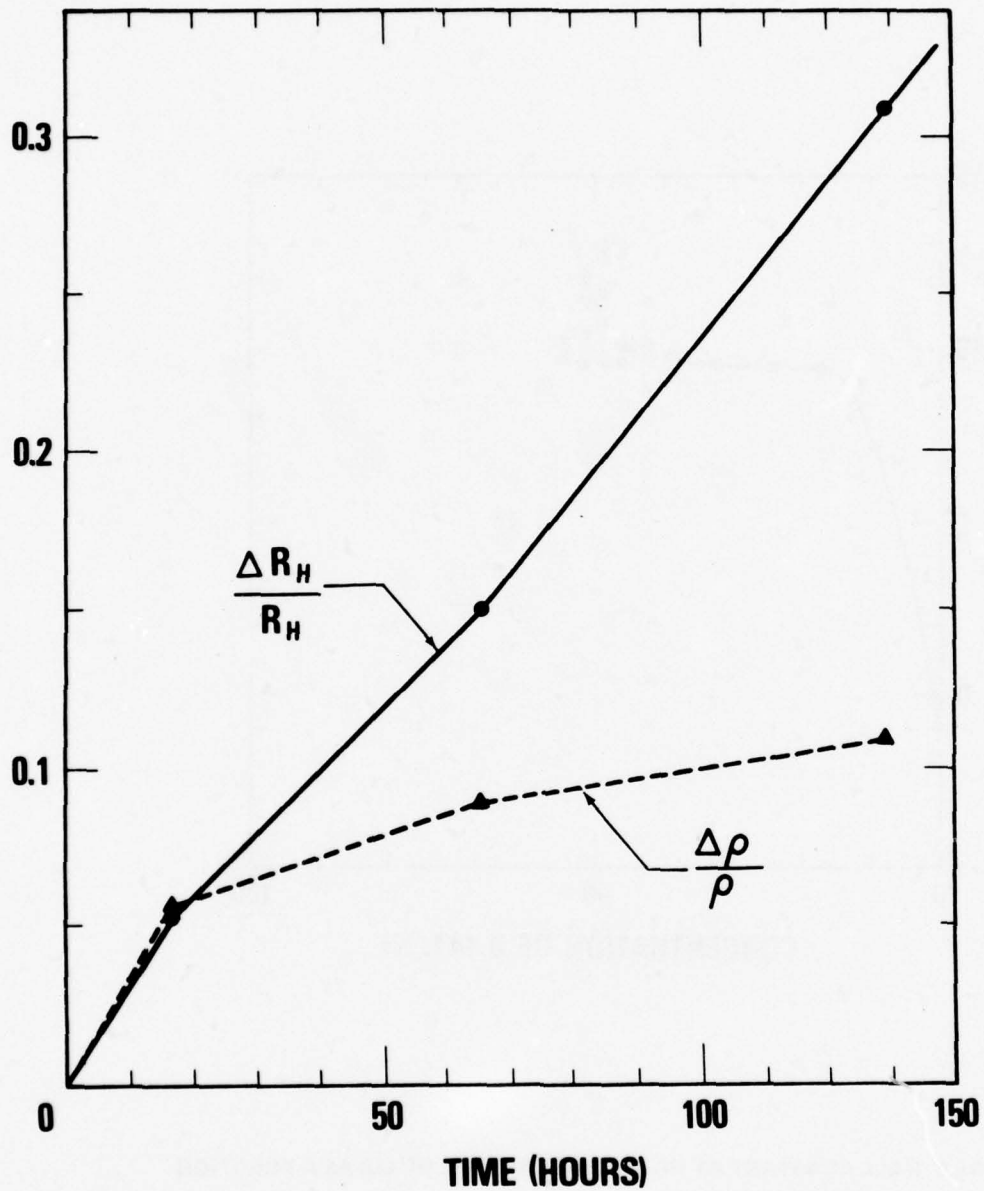


FIGURE 6 DEGRADATION OF A 39.1B SAMPLE IN THE HERMETICALLY SEALED SAMPLE HOLDER AS A FUNCTION OF TIME AT ROOM TEMPERATURE.

TABLE 2
COMPARISON OF ELECTRICAL DATA^a

Compound	R_H	Resistivity	Hall Mobility	Carrier Conc.
	$(10^{-10} \text{ m}^3/\text{C})$	ρ $(10^{-8} \Omega\text{m})$	μ $(10^{-2} \text{ m}^2/\Omega\text{C})$	N (Calc) (10^{29} m^{-3})
Cu	-0.55	1.70	3.23	-1.13
Rh	370	4.78	77.4	1.69×10^{-3}
Ta	1.01	13.1	$7.7_1 \times 10^{-2}$	0.61_8
Li	-1.7	9.21	0.18_4	-0.36_7
B^b	$(2.8 \pm 2.3) \times 10^9$	1.7×10^{14}	$1.6_4 \times 10^{-5}$	$2.2_3 \times 10^{-10}$
$Li_x B_{1-x}^c$	9.5 to 13	12.5 to 23	0.76 to 0.57	$(6.6 \text{ to } 4.8) \times 10^{-2}$

^a Room temperature

^b Semiconductor, $E_g = 1.6 \text{ eV}$

^c $x = 0.80 \text{ to } 0.50 \text{ at. fraction}$

The temperature dependence of the electrical resistivity of the alloys is plotted in Fig. 7. The increase of electrical resistivity with B concentration is again quite pronounced (as in Fig. 4). The data for pure Li were taken from reference 11. The low temperature data for 50B (solid points) are probably a bit high as the sample was not well protected from contamination by H₂O, O₂, and N₂.

In general, the electrical resistivity is typical of a metallic alloy, i.e., there is a temperature independent part at the lowest temperatures, and a temperature-dependent part which increases with increasing temperature. Mathiessen's rule is not even approximately obeyed. Since B is a semiconductor, it is not unreasonable to expect that one of the compounds of LiB will be semiconducting, although none of the alloys we have measured have a positive temperature coefficient ($-\frac{1}{\rho} \frac{d\rho}{dT}$). The most interesting feature of Fig. 7 is the break in the curve of the 40B sample at the melting point of Li at 454°K, and the fact that it does not occur in the 50B sample. This would indicate that there is a significant amount of free Li in the 40B sample, but not in 50B. It is of interest to try to calculate how much free Li there is in the 40B.

To do this make the simplifying assumption that there are two geometrically simple resistances in parallel in the 40B sample, one of pure Li and the other containing the various LiB phases. Define

$$\beta \equiv \rho_+ / \rho_- = R_+ / R_-$$

$$\gamma \equiv \rho_{L+} / \rho_- = R_{L+} / R_-$$
(1)

where ρ and ρ_L are the electrical resistivities of the sample and of pure Li, respectively; R and R_L are the electrical resistances of the sample and of the pure Li in the sample, respectively; and the + and - refer to values just above the just below the melting point of Li, respectively. The β and γ may be obtained from Fig. 7. Suppose R_x is the resistance of the LiB phases in 40B and that resistance of pure Li and R_x add in parallel. Then

$$R_- = \frac{R_x R_L}{R_x + R_L}$$

$$R_+ = \frac{R_x R_L}{R_x + R_{L+}}$$
(2)

Define:

$$\alpha \equiv R_x / R_{L+}$$
(3)

11. Shipil'rain, E. E. and Savchenko, V. A., "Experimental Study of the Electrical Conductivity of Lithium and Cesium in the Condensed Phase at Temperatures up to 1200°K," Teplofizika Vysolikh Temperatur, 6, 254 (1968).

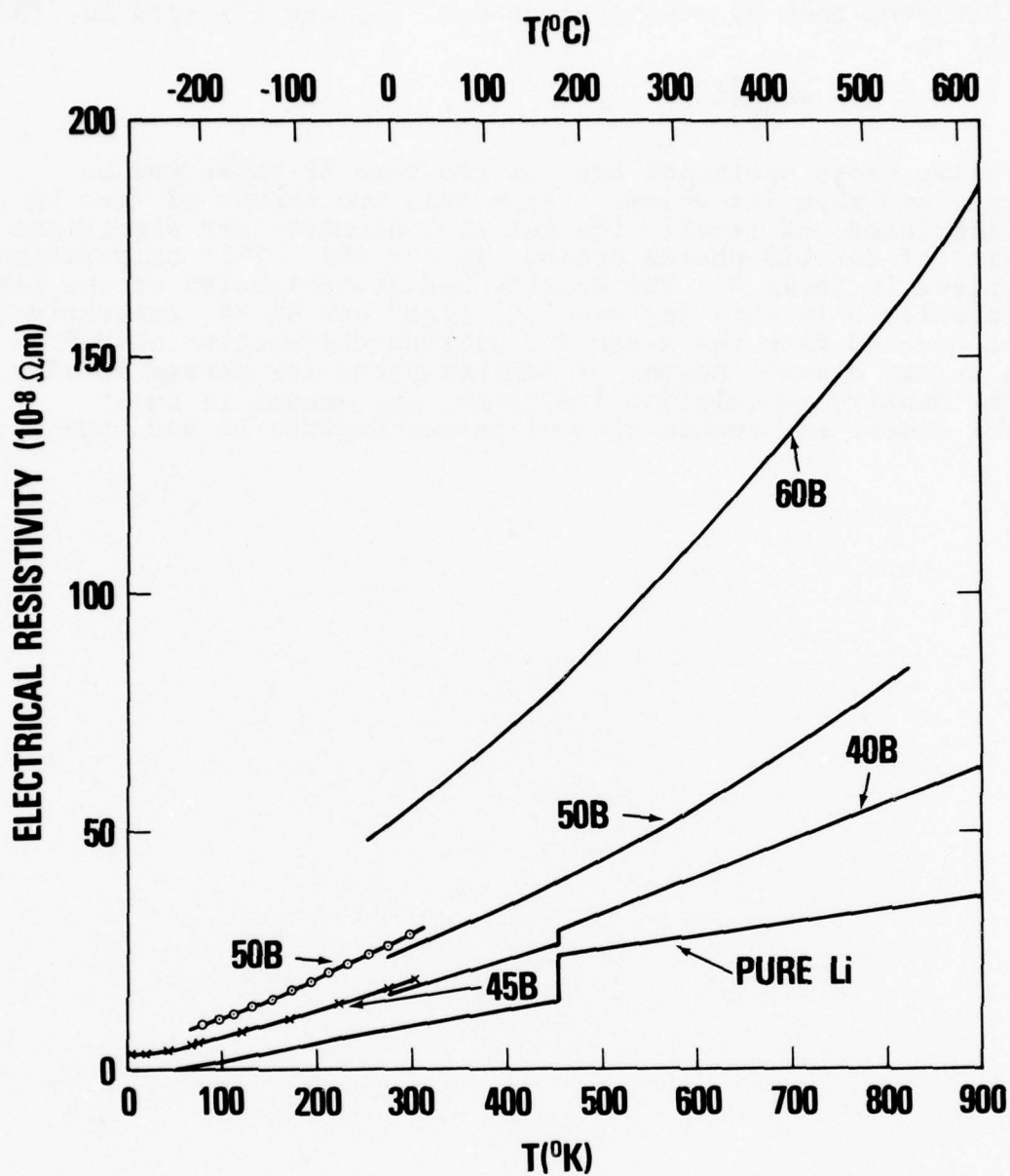


FIGURE 7 ELECTRICAL RESISTIVITY OF LiB ALLOYS AS A FUNCTION OF TEMPERATURE.

The two constants β and γ are to be determined from Fig. 7, and α can be obtained from them by substituting Eqs. (1) and (3) into Eq. (2). The result is

$$\alpha = \frac{\gamma(\beta-1)}{\gamma+\beta}$$

The effective cross sectional area of the pure Li phase may be calculated, and then its volume. From this the amount of free Li may be calculated and finally the net stoichiometry and electrical resistivity of the LiB phases present in the 40B. This calculation is summarized in Table 3. The density and stoichiometry of the LiB phases calculated in this way are 1.07 g/cm³ and 44.7B, respectively, which are deduced from the x-ray and neutron diffraction study⁶. There is surely a small amount of another phase (or phases) present, but as the density calculation indicates, the amount is small ($\cong 3\%$, for almost any combination of phases besides Li and Li₅B₄).

TABLE 3

CALCULATION OF STOICHIOMETRY OF PHASE I IN 40B SAMPLE

Symbol	Explanation	Value	Units
R_+	Electrical resistance of sample above M.P.*	1.02	m Ω
R_-	Electrical resistance of sample below M.P.*	0.91	m Ω
ρ_{L+}	Electrical resistivity of pure Li above M.P.*	23.7	$\mu\Omega$
ρ_{L-}	Electrical resistivity of pure Li below M.P.*	14.62	$\mu\Omega$
a	Sample width	3.345	mm
b	Sample thickness	1.643	mm
ℓ	Sample length	51.6	mm
L	Voltage probe spacing	19.0	mm
β	R_+/R_-	1.12 ₁	
γ	ρ_{L+}/ρ_{L-}	1.62 ₁	
α	$\gamma(\beta-1)/(\gamma-\beta)$	0.39 ₁₈	
R_{L-}	Resistance of pure Li in sample below M.P.*	3.23 ₃	m Ω
A_L	Effective cross section of pure Li phase in sample	0.8593	(mm) ²
V_L	Volume of pure Li phase in sample	44.34	(mm) ³
d_L	Density of pure Li	0.534	gm/cm ³
W	Total weight of sample	0.280	gm
ΔW_L	Weight of pure Li phase in sample	0.023 ₇	gm
W_L	Total weight of all Li in sample	0.137	gm
W_B	Total weight of all B in sample	0.142	gm
R_X	Resistance of LiB phases in sample at M.P.*	1.30 ₂	m Ω
ρ_X	Resistivity of LiB phases at M.P.*	31.8	$\mu\Omega$ cm
d_s	Density of sample	0.98 ₇	gm/cm ³
d_w	Density of LiB phases in sample	1.07	gm/cm ³
ρ_-	Electrical resistivity of sample just below M.P.*	26.3	$\mu\Omega$ cm
	Electrical resistivity of LiB phases at 300°K	20.5	$\mu\Omega$ cm
a_L	Atomic percent of Li in LiB phases	55.3	a/o

* M.P. = Melting point of pure Li (180.5°C)

DENSITY RESULTS

The measured density of the LiB alloys as a function of composition is plotted in Fig. 8. The error in density resulting from errors in the weight and volume measurements is less than 0.5%. Above 30B porosity was a serious problem, as the X's in Fig. 8 indicate. The X's are samples whose volume was not constrained in a mold during solidification of the alloy, while the circles with slashes represent samples whose volume was constrained during the solidification process. The theoretical density of Li_5B_4 , calculated using the stoichiometry and lattice spacing, is indicated by the + in Fig. 8. The density increases rapidly as the concentration of B increases, which is to be expected since the density of B is 4-5 times higher than Li^6 .

DENSITY, DISCUSSION AND INTERPRETION. A fair amount of information can be gleaned from Fig. 8 concerning the phases present in the alloys and it would appear that there are more than 2 (i.e., these alloys are not at thermodynamic equilibrium). Suppose there are n phases present

$$[\text{Li}_{x_1}\text{B}_{1-x_1}]z_1 + [\text{Li}_{x_2}\text{B}_{1-x_2}]z_2 + \cdots + [\text{Li}_{x_n}\text{B}_{1-x_n}]z_n$$

where $0 \leq x_i \leq 1$ and $0 \leq z_i \leq 1$. Assume that the stoichiometries, the x_i 's, and the densities, and d_i 's, of the phases are known. We want to find out if these phases can coexist stoichiometrically and also give the composite density, or, to put it in another way, to find a realistic set of z_i 's. Stoichiometry requires that

$$z_1 + z_2 + \cdots + z_n = \sum_{i=1}^n z_i = 1.0 \quad (4)$$

$$x_1z_1 + x_2z_2 + \cdots + x_nz_n = \sum_{i=1}^n x_iz_i = c \quad (5)$$

where c is the total concentration of Li in the alloy. The density of the alloy with n phases may be derived in terms of the densities of the phases present in the following way. The total density is the total weight of the alloy, W, divided by the sum of the volumes of n phases present. The volume V_i of the i^{th} phase is

$$V_i = \frac{[W_{\text{Li}}]_i + [W_{\text{B}}]_i}{d_i}$$

where $[W_{\text{Li}}]_i$ and $[W_{\text{B}}]_i$ are the weights of Li and B, respectively,

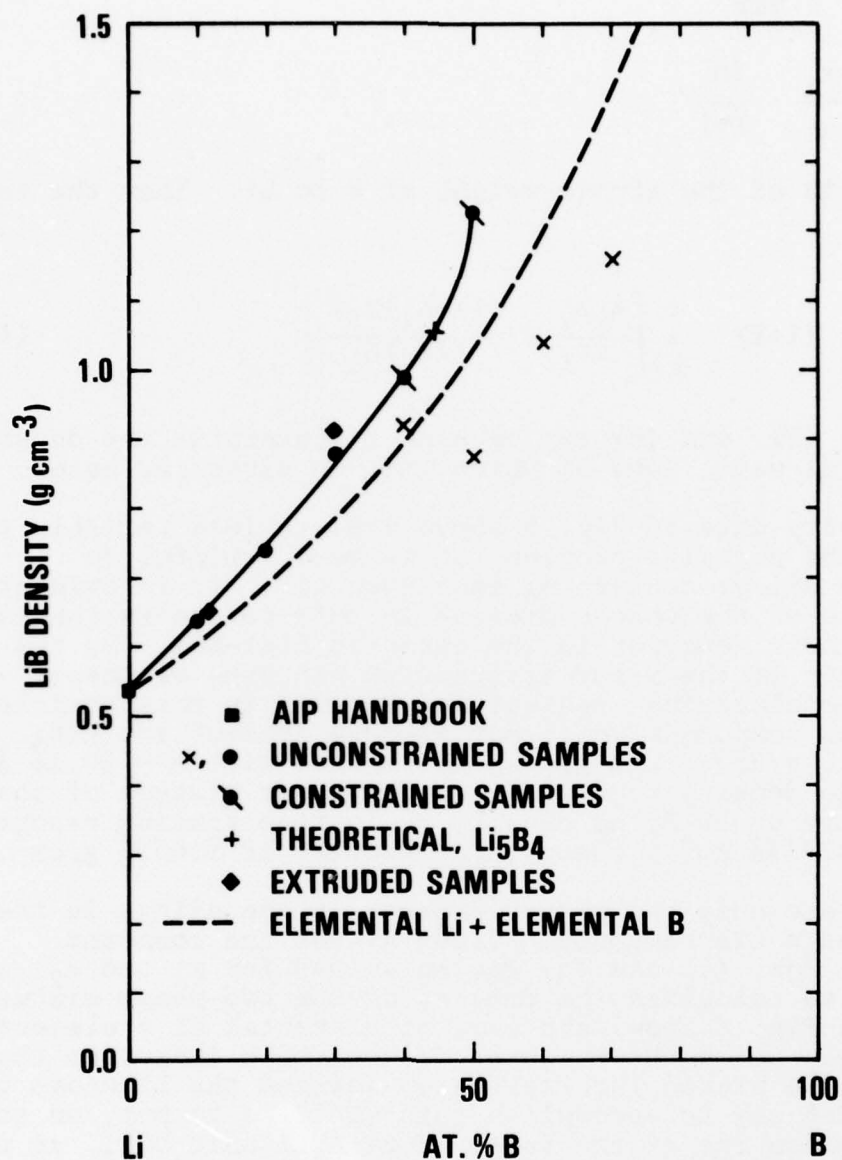


FIGURE 8 DENSITY OF LiB ALLOYS AS A FUNCTION OF CONCENTRATION OF B. THE SOLID CURVE IS DRAWN THROUGH THE DATA POINTS. THE DASHED CURVE IS CALCULATED ASSUMING A MIXTURE OF FREE Li AND FREE B.

present in the i^{th} phase. These are given by

$$[W_{\text{Li}}]_i = \frac{x_i z_i}{c} \cdot \frac{W}{1+f}$$

$$W_{B i} = z_i \frac{1-x_i}{1-c} \cdot \frac{Wf}{1+f}$$

where f is the ratio of the atomic weight of B to Li. Then the total density is

$$d = \frac{W}{\sum_{i=1}^n V_i} = (1+f) \left[\sum_{i=1}^n \left[\frac{x_i z_i}{c d_i} + \frac{(1-x_i) z_i f}{(1-c) d_i} \right] \right]^{-1} \quad (6)$$

Equations (4), (5), and (6) can be used to interpret the density of Fig. 8 in several ways, some of which will be discussed below.

Since the density data in Fig. 8 above 45B are less reliable than below because of the porosity problem, it is more fruitful to concentrate on the alloys containing less than 45B. It is evident that pure Li is one of the phases present in this concentration range, as shown by the anodic behavior in the eutectic LiCl-KCl,⁷ by the presence of Li lines in the x-ray diffraction patterns of these alloys⁸, and by the electrical resistivity earlier in this article. Previously reported compounds which may also be present are LiB₄, $a = 7.20 \text{ \AA}$, $d = 1.73 \text{ g/cm}^3$;³ LiB_{10±.35}, tetragonal with $a = 10.16 \text{ \AA}$ and $c = 14.28 \text{ \AA}$ (no density reported);⁴ a phase, or mixture of phases, with a stoichiometry of Li₂B, no density or lattice spacing reported⁷; and Li₅B₄ with a 4.935 \AA and a theoretical density of 1.0537 g/cm^3 .⁸

Suppose there are only two phases present in the alloys in the 0-40B range, Li and a LiB compound. Given x_2 for the compound ($x_1 = 1.0$ for Li), Eqs. (4) and (5) can be solved for z_1 and z_2 , and then Eq. (6) used to calculate the density of the two-phase mixture. The dashed line in Fig. 8 shows the case of elemental Li + elemental B. It lies considerably below the measured values which indicates that B atoms must somehow be packed interstitially between the Li atoms in the Li lattice. One way to accomplish this would be to put, on the average, one B atom on one of the faces of each Li unit cell, as will be shown shortly (or statistically, 1/3 B atom on each face). The important conclusion to be drawn here is that there cannot be a significant amount of elemental B present in the alloys -- there must be other phases present.

Table 4 shows some of the possible simple LiB compounds. The atomic diameter of pure Li is about 3.04 \AA and that of B is 1.96 \AA , but the latter is found to vary substantially in compounds. The compounds in Table 4 marked with an * are based on packing of Li and B spheres

TABLE 4

POSSIBLE LiB COMPOUNDS

Compound	c (at.fr.Li)	Struct.	a (Å)	Calc. Density (g/cm ³)	Density per at.fr.Li
B	0.00	--	---	2.535 ^a	--
*LiB ₆ ^b	0.143	cubic	3.51	2.72	19.04
*Li ₉ B ₄₂	0.177	cubic	7.0	2.45	13.88
LiB ₄	0.200	cubic	7.20	1.73	8.65
*Li ₁₂ B ₂₄	0.333	cubic	7.0	1.62	4.86
*Li ₂ B ₃	0.400	bcc	3.51	1.74	4.35
*Li ₄ B ₄	0.500	fcc	4.935	0.960	1.92
Li ₅ B ₄ ^c	0.556	rh. (c.)	4.935	1.054	1.90
*Li ₆ B ₃	0.667	cubic	4.935	1.001	1.50
*Li ₂ B	0.667	hcp	3.11 (c = 5.09)	0.942	1.41
*Li ₂ B ^d	0.667	cubic	3.51	0.928	1.39
*Li ₃ B	0.75	cubic	3.51	1.189	1.59
Li	1.00	bcc	3.51	0.534 ^a	0.53

*Structures derived from packing of Li and B spheres

^aMeasured densities from AIP Handbook

^bLithium hexaboride; analogous to LaB₆

^cDerived from a consideration of the X-ray and Neutron Diffraction patterns of the polycrystalline alloys.

^dBoron interstitial, on face of bcc cell.

with the above diameters. Fig. 9 shows a comparison of the density calculated with Eq. (6) for a binary mixture of elemental Li and one of these compounds with the measured density (d_m). The compounds which give the best fit are $\text{Li}_2\text{B}(\text{cub})$ and $\text{Li}_2\text{B}(\text{hcp})$. However, the structure of either of these two compounds in combination with Li cannot index the observed x-ray diffraction pattern.

None of the other binary phase mixtures fit the observed density, as Fig. 9 shows, and in any case it is highly likely that there are more than two phases present in the alloy between 0 and 45B. There is metallographic evidence for three¹². One other interesting feature is that the compounds with the lowest density per atomic fraction of Li, the last column in Table 4, seem to give the best results for density, as Fig. 9 shows.

Suppose now that there are 3 phases present. Then, Eqs. (4), (5), and (6) are three equations in three unknowns, z_1 , z_2 , and z_3 , assuming that we know the stoichiometry and density of the three and setting $d = d_m$ in Eq. (6). The Li_5B_4 phase is likely to be present, in addition to Li. The only phase in Table 2 which, in combination with Li and Li_5B_4 , can yield a set of solution to Eqs. (4), (5), and (6) in the composition range 0-40B is Li_3B . Those solutions are given in Table 5. The fifth column shows the atomic percent of Li present in the $\text{Li}_5\text{B}_4 + \text{Li}_3\text{B}$ combination. These compare well with the 67 at % Li found in the electrochemical test of 13.8B and 31.6B alloys⁷.

The above type of analysis can be extended to four or more phases, in which case there are 3 equations in 4 or more unknown z_i 's. In general, there will be a range of z_i for each i th phase. There is not much to be gained by going through this exercise exhaustively. However, three different combinations were tried, $\text{Li} + \text{Li}_5\text{B}_4 + \text{LiB}_4 + \text{Li}_2\text{B}$, $\text{Li} + \text{Li}_5\text{B}_4 + \text{LiB}_6 + \text{Li}_3\text{B}$, and $\text{Li} + \text{Li}_5\text{B}_4 + \text{Li}_3\text{B} + \text{LiB}_4$. Only the latter yielded a realistic set of solutions with z_4 (for LiB_4) allowed to vary from 0 to about 0.4 in the total composition range of 0-40B.

Some important information has emerged from the above somewhat tedious analysis. The main points are: (1) the LiB cannot simply be a mixture of elemental Li and elemental B; (2) some of the phases present in the alloy composition range 0-40B must have a closer packing of Li than in the bcc Li structure; (3) there are probably 3 or more phases present which means that the alloys considered are not equilibrium binary alloys; (4) the coexistence of the 3 phases, Li, Li_5B_4 , and Li_3B , is supported by all of the density calculations.

That the electrical properties of these alloys are subject to some experimental uncertainty because of their undetermined and variable metallurgical nature should not be surprising.

12. Ernst, Donald, Dr., Naval Surface Weapons Center, private commun.

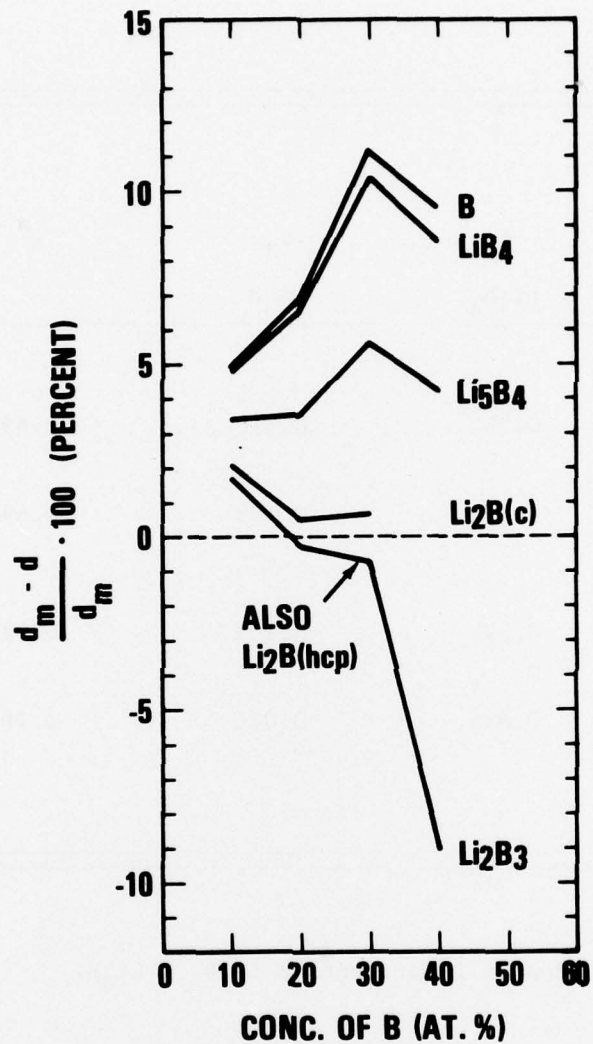


FIGURE 9 PERCENTAGE DIFFERENCE BETWEEN THE MEASURED DENSITY, d_m , AND THE CALCULATED DENSITY, d , OF A MIXTURE OF Li WITH A SECOND PHASE (LABELED NEXT TO THE CURVE). THE Li_2B AND Li_2B_3 ARE HYPOTHETICAL PHASES.

TABLE 5

COMPOSITION OF LiB WITH 3 PHASES PRESENT, Li, Li_5B_4 AND Li_3B

c	z_1	z_2	z_3	x^a
Total Li	Free Li	Li_5B_4	Li_3B	
0.900	0.727	0.163	0.110	0.634
0.800	0.505	0.392	0.103	0.596
0.700	0.260	0.591	0.149	0.593
0.600	0.088	0.885	0.026	0.561

$$^a x = \frac{x_2 z_2 + x_3 z_3}{z_2 + z_3} \quad . \quad \text{Atomic fraction of Li present in } \text{Li}_5\text{B}_4 + \text{Li}_3\text{B}.$$

CONCLUSIONS

The only LiB compounds reported previous to 1972 were the B rich phases LiB_6 , $\text{Li}_{32}\text{B}_{68}$; LiB_4 ; and $\text{LiB}_{10.85}$. In 1972 a whole new class of LiB alloys was discovered that included many possible Li rich compounds, one of which is Li_5B_4 . The unique way in which these compounds are formed makes the control and understanding of the properties difficult.

Densities, electrical resistivities and Hall coefficients of these new LiB alloys have been presented here. Since the phase diagram of LiB is not known, much of this work was directed toward understanding the metallurgical nature of the alloy.

From an analysis of the density made by calculating the theoretical density of the alloy from the known stoichiometry and density of the various phases present several conclusions are possible. (1) It is known that free Li is present in the composition range 0-40B, from the electrochemical work⁷, from the structure work⁸, and from the resistivity data presented here. Since the density calculated for a combination of elemental Li and elemental B is too low, there cannot be a significant amount of free B, and there must be another phase, or phases, present. (2) The phases present must have a closer packing of Li than in the bcc Li structure. Hexagonal Li could account for this, but such a structure does not index the observed x-ray diffraction pattern. (3) There are probably 3 or more phases present in the alloys studied, which means the alloys were not in thermodynamic equilibrium. (4) The three coexistent phases, Li, Li_5B_4 , and Li_3B could explain both the density and observed x-ray results.

The electrical resistivity of the alloys at room temperature is fairly constant between 0 and 45B, after which it increases rapidly. This behavior could be expected since the electrical resistivity of B is about 12 orders of magnitude higher than Li.

The Hall constant at room temperature doesn't vary much with composition between 10 and 50B and has a magnitude of about $10^{-9}\text{m}^3\text{C}^{-1}$. Lithium has $R_H = -1.7 \times 10^{-10}\text{m}^3\text{C}^{-1}$, and B has a large, positive Hall constant. Above 50B the Hall constant of the alloy increases more rapidly.

A study of the degradation of the samples due to contamination by the impurities H_2O , O_2 , and N_2 suggests that the compounds of LiB are more susceptible to corrosion than pure Li.

The temperature dependence of the electrical resistivity of these alloys is metallic in nature; and the magnitude is low, that of a well conducting metallic alloy. No indication of semiconducting behavior was found, although there was a rapid rise of resistivity as the B concentration increased above 50B. The temperature dependence of 3 samples, 40B, 50B, and 60B was studied above room temperature.

There was a 10% break in the resistivity of the 40B sample at the melting point of Li, which indicated the presence of free Li in that alloy. It was possible from the size of the break to estimate that the concentration of Li and the density of LiB phases in the 40B sample were 55.3 at.% and 1.07 g/cm³, respectively, very close to the stoichiometry and density of Li₅B₄, i.e., 55.6 Li and 1.0537 g/cm³, respectively.

No correlation of properties with different annealing treatments was found. It is thought that the properties are determined by the mixture of phases present.

REFERENCES

1. Elliott, R. P., Constitution of Binary Alloys, First Supplement, (McGraw-Hill, New York, 1965), p. 124.
2. Shunk, F. A., Constitution of Binary Alloys, Second Supplement, (McGraw-Hill, New York 1969), p. 89.
3. Casanova, J. French Patent No. 1,461,878 (1965).
4. Secrist, D. R., "Compound Formation in the Systems Lithium-Carbon and Lithium-Boron," J. Amer. Cer. Soc., 50, 520 (1967)
5. Wang, F. E., "Unusual Phenomenon in the Formation of Li-B Compound Alloy," Naval Surface Weapons Center, White Oak Laboratory, submitted to Phys. Rev. Ltrs.
6. Gray, Dwight E., American Institute of Physics Handbook, Third Ed., (McGraw-Hill, New York, 1972), pps. 2-19, 2-20.
7. James, S. D. and Devries, L. E., "Structure and Anodic Discharge Behavior of Lithium-Boron Alloys in the LiCl-KCl Eutectic Melt," J. Electrochem. Soc., 123, 321 (1976)
8. Wang, F. E., "The Crystal Structure Study of Li_5B_4 ," NSWC/WOL TR 77-84, (ONR Report No. N-0014-WR0030), 1977.
9. Mitchell M. A., A Simple Resistance Probe for Measurements from 4.2 to 300K," Rev. Sci. Inst., 45, 708 (1974).
10. Mitchell, M. A., "A Simple Microohmmeter," submitted for publication in Rev. Sci. Inst.
11. Shipl'rain, E. E. and Savchenko, V. A., "Experimental Study of the Electrical Conductivity of Lithium and Cesium in the Condensed Phase at Temperatures up to 1200°K," Teplofizika Vysolikh Temperatur, 6, 254 (1968).
12. Ernst, Donald, Dr., Naval Surface Weapons Center, private commun.

ACKNOWLEDGEMENTS

The authors gratefully acknowledge the help and advice of Dr. Frederick Wang and Dr. Donald Ernst in the course of this work, and we appreciate the use of some of their unpublished data. This work was supported by Bruce MacDonald of ONR under Contract No. N00014-7TWR-T0030.

The authors also gratefully acknowledge the assistance of the REVMAT Program.

DISTRIBUTION LIST

Copies

Office of Naval Research
Department of the Navy
Washington, D. C. 20360
Code 471
Code 102
Code 470

Commanding Officer
Office of Naval Research
Branch Office
495 Summer Street
Boston, Massachusetts 02210

Commanding Officer
Office of Naval Research
Branch Office
536 South Clark Street
Chicago, Illinois 60605


Office of Naval Research
San Francisco Area Office
760 Market Street, Room 447
San Francisco, California 94102
Dr. P. A. Miller

Commander
Naval Research Laboratory
Washington, D. C. 20375
Code 6000
Code 6100
Code 6300
Code 6400
Code 2627

Commanding Officer
Naval Air Development Center
Warminster, Pennsylvania 18974
Code 302, Mr. F. S. Williams

Commanding Officer
Naval Air Propulsion Test Center
Trenton, New Jersey 08628
Library

Commanding Officer
Naval Construction Battalion
Civil Engineering Laboratory
Port Hueneme, California 93043
Materials Division



DISTRIBUTION LIST (Cont.)

Copies

Commanding Officer
Naval Ocean Systems Center
San Diego, California 92152
Electron Materials
Sciences Division
Library

Commanding Officer
Naval Missile Center
Materials Consultant
Code 3312-1
Point Mugu, California 93041

David W. Taylor Naval Ship R&D Center
Annapolis, Maryland 21402
Materials Department

Naval Underwater System Center
Newport, Rhode Island 02840
Library

Naval Postgraduate School
Monterey, California 93940
Mechanical Engineering Dept.

Commander
Naval Air Systems Command
Washington, D. C. 20360
Code 52031
Code 52032
Code 320

Commander
Naval Sea Systems Command
Washington, D. C. 20362
Code 035

Commanding Officer
Naval Facilities Engineering Command
Alexandria, Virginia 22331
Code 03

Scientific Advisor
Commandant of the Marine Corps
Washington, D. C. 20380
Code AX

DISTRIBUTION LIST (Cont.)

Copies

Naval Ship Engineering Center
CTR BG #2
3700 East-West Highway
Prince Georges Plaza
Hyattsville, Maryland 20782
Engineering Materials and
Services Office, Code 6101

Office of Chief of Research &
Development
Department of the Army
Energy Conversion Branch
Room 416, Highland Bldg.
Washington, D. C. 20315

Army Research Office
Box CM, Duke Station
Durham, North Carolina 27706
Metallurgy & Ceramics Div.

Army Materials and Mechanics
Research Center
Watertown, Massachusetts 02172
Res. Programs Office (AMXMR-P)

Air Force
Office of Scientific Research
Bldg 410
Bolling Air Force Base
Washington, D. C. 20332
Chemical Science Directorate
Electronics and Solid State
Sciences Directorate

Air Force Materials Lab (LA)
Wright-Patterson AFB
Dayton, Ohio 45433

NASA Headquarters
Washington, D. C. 20546
Code RRM

National Aeronautics and Space
Administration
Goddard Space Flight Center
Greenbelt, Maryland 20771

NASA, Lewis Research Center
21000 Brookpark Road
Cleveland, Ohio 44135
Library

DISTRIBUTION LIST (Cont.)

Copies

National Bureau of Standards
Washington, D. C. 20234
Metallurgy Division
Inorganic Materials Division

Defense Metals and Ceramics
Information Center
Battelle Memorial Institute
505 King Avenue
Columbus, Ohio 43201

Director
Ordnance Research Laboratory
P. O. Box 30
State College, Pennsylvania 16801

Director, Applied Physics Laboratory
University of Washington
1013 Northeast 40th Street
Seattle, Washington 98105

Metals and Ceramics Division
Oak Ridge National Laboratory
P. O. Box X
Oak Ridge, Tennessee 37380

Los Alamos Scientific Laboratory
P. O. Box 1663
Los Alamos New Mexico 87455
Report Librarian
Dr. C. Y. Huang, MS-704

Argonne National Laboratory
Metallurgy Division
P. O. Box 229
Lemont, Illinois 60439

Argonne National Laboratory
9700 South Cass Avenue
Argonne, Illinois 60439
Mr. A. A. Chilenskas

Brookhaven National Laboratory
Technical Information Division
Upton, Long Island, New York 11973
Research Library

Library
Building 50, Room 134
Lawrence Radiation Laboratory
Berkeley, California 94704

DISTRIBUTION LIST (Cont.)

Copies

Professor Y. N. Chiu
Department of Chemistry
Catholic University
Washington, D. C. 20017

Professor W. N. Lipscomb
Chemistry Department
Harvard University
Cambridge, Massachusetts 02138

Professor F. A. Kanda
Chemistry Department
Syracuse University
Syracuse, New York 13210

Professor C. W. Kern
Department of Chemistry
Ohio State University
140 West 18th Avenue
Columbus, Ohio 43210

Naval Sea Systems Command
Washington, D. C. 20360
Attn: SEA-09G32
SEA-03B

2

Defense Documentation Center
Cameron Station
Alexandria, Virginia 22314

12